Supporting Information

Detection and Structural Characterization of Ether Glycerophosphoethanolamine from Cortical Lysosomes Following Traumatic Brain Injury Using UPLC-HDMS^E

Jace W. Jones[1], Chinmoy Sarkar[2], Marta M. Lipinski[2], Maureen A. Kane[1*]

[1]University of Maryland, School of Pharmacy, Department of Pharmaceutical Sciences, Baltimore, MD; [2]University of Maryland, School of Medicine, Department of Anesthesiology, Baltimore, MD

[*]Correspondence: Maureen A. Kane, PhD: 20 N. Pine St, N731; Baltimore, MD 21201. 410-706-5097(p), 410-706-0886 (f), mkane@rx.umaryland.edu

Table of Contents

Table S-1: Differentially expressed brain lysosomal ether PE lipids after TBI.

Materials and Methods

Animal Model of Traumatic Brain Injury

The animal model of traumatic brain injury (TBI) used has been described previously (Sarkar C et al, 2014; Sarkar C, et al, 2018). All surgical procedures and animal experiments were performed in accordance with the protocols approved by the Animal Care and Use Committee of the University of Maryland. Briefly, controlled cortical impact (CCI) induced TBI was performed in male C57BL6/J mice (20-25g) where a 10-mm midline incision was made over the skull, the skin and fascia were retracted and a 4-mm craniotomy was made on the central aspect of the left parietal bone of mice under surgical anesthesia (2-3% isoflurane evaporated in a gas mixture containing 70% N_2O and 30% O_2). Moderate injury was induced by a custom microprocessor-controlled and compressed air driven pneumatic impactor of 3.5 mm diameter tip with the impact velocity of 6 m/s and a deformation depth of 2 mm. In sham animals, same procedure was performed except for the impact. Lysosomes were isolated from mouse brains (cortical tissue) at 1 h post-injury via subcellular fractionation and further enriched using density gradient centrifugation (Lysosomal purification kit; Thermo Scientific cat # 89839) as described previously (Sarkar C, et al., 2018). Isolated lysosomes were stored at -80 °C until assay.

References for Animal Model:

Sarkar, C., Zhao, Z., Aungst, S., Sabirzhanov, B.*, et al.*, Impaired autophagy flux is associated with neuronal cell death after traumatic brain injury. *Autophagy* 2014, *10*, 2208-2222.

Sarkar, C., Jones, J. W.*, Hegdekar, N.*, Thayer, J. A.*, et al.*, cPLA2 mediated lysosomal membrane damage leads to inhibition of autophagy and neurodegeneration after brain trauma. *submitted* 2018. * equal contributions.

MTBE Lipid Extraction Protocol

Total lipid extracts from the lysosome samples were prepared using a MTBE lipid extraction protocol by Matyash et al. with slight modifications. Briefly, 400 µL of methanol (ice cold) was added to the lysosome fraction. 10 µL of internal standard mixture (Splash Lipidomix, Avanti Polar Lipids, Alabaster, AL) and 500 µL of MTBE (ice cold) were added followed by 1 hour incubation on ice with occasional vortex mixing. 500 µL of water (ice cold) was added slowly and incubated on ice for 15 minutes with occasional vortex mixing. Phase separation was completed by centrifugation at 5,000 RPM for 5 min at 4 °C. The upper, organic phase was removed and set aside on ice. The bottom, aqueous phase was re-extracted with 200 µL of MTBE followed by 10 minutes of incubation on ice with occasional vortex mixing. Phase separation was completed by centrifugation at 5000 RPM for 5 min at 4 °C. The upper, organic phase was removed and combined with previous organic extract. The organic extract was dried under a steady stream of nitrogen at 30 °C. The recovered lipids were reconstituted in 500 uL of chloroform:methanol (1:1, v/v) containing 200 µM of butylated hydroxytoluene. Prior to analysis samples were further diluted 5 fold with acetonitrile:isopropanol:water (65:30:5, v/v/v).

Reference for MTBE Lipid Extraction Protocol:

Matyash, V., Liebisch, G., Kurzchalia, T. V., Shevchenko, A., Schwudke, D., Lipid extraction by methyl-tert-butyl ether for high-throughput lipidomics. *Journal of lipid research* 2008, *49*, 1137-1146.

Results and Discussion

HDMS^E for Structure Identification for Alkyl Ether PE

The identification of alkyl ether PE (PE-O) followed a similar workflow as described for vinyl ether PE. The first step involved accurate mass database searching of precursor ions within a given experimental mass accuracy tolerance to narrow the search to all possible PE candidates. This was followed by cross-referencing potential PE candidates to chromatographic retention and HDMS^E (both positive and negative ion mode) mass spectra. The result of this process yielded confident structure assignment.

An example of this workflow can be seen in the structure elucidation of the alkyl ether PE: PE(O-16:0/22:6). Database searching (≤7.5 ppm window) of the precursor ions at *m/z* 748.5290 (negative; t_R=9.4 min) and 750.5418 (positive; t_R=9.4 min) resulted in two possible lipid candidates: PE(O-38:6) and PE(P-38:5). The negative ion mode HDMS^E elevated-collision energy mass spectrum resulted in characteristic product ions that confidently assigned the *sn*-2 position as a 22:6 acyl chain (SI Figure S-6A). These product ions corresponded to the neutral loss of the *sn*-2 acyl chain (*m/z* 438.3; -22:6ket) and charge retention at the *sn*-2 acyl chain (*m/z* 327.2; $[22:6]^-$) followed by a consecutive dissociation of carbon dioxide (*m/z* 283.2; $[22:6 – COO]^-$). The consecutive loss of carbon dioxide from a docosahexanoic acid anion ($[22:6]^-$) is commonly reported for CID of GPL containing a *sn*-2 22:6 acyl chain [reference 26 main text]. The product ion at *m/z* 283.2 could arise from an intact $[18:0]^-$ acyl chain but the accurate mass difference between $[22:6\text{-}COO]^-$ (*m/z* 283.2431) and $[18:0]^-$ (*m/z* 243.2643) precludes this as a possibility. Of note similar to vinyl ether PE, alkyl ether PE does not readily dissociate at the *sn*-1 position in CID. This was confirmed here and in direct contrast to diacyl PE where competitive fragmentation at both the *sn*-1 and *sn*-2 positions are common (SI Figure S-4).

By deductive reasoning if the *sn*-2 position houses a 22:6 acyl chain and there are two possible candidate structures according to accurate mass ((PE(O-38:6) and PE(P-38:5)) then the *sn*-1 position by default is alkyl ether, O-16:0. This would assign the *m/z* values at 748.5290 (negative; t_R=9.4 min) and 750.5418 (positive; t_R=9.4 min) to a lipid structure of PE(O-16:0/22:6). Further confirmation for distinguishing between the alkyl ether and vinyl ether PE is seen in the positive ion mode HDMS^E mass spectrum (SI Figure S-6B). The only product ion observed in the positive ion mode CID mass spectrum of *m/z* 750.5418 was the neutral loss of the PEtN head group. The neutral loss of PEtN is the dominant fragmentation channel for diacyl PE (SI Figure S-4) and alkyl ether PE (SI Figure S-6B) yet is of low relative abundance for vinyl ether PE (Figure 3, SI Figure S-5B). The presence of the dominant PEtN dissociation channel and absence of diagnostic vinyl ether product ions (Figure 3) confirms the alkyl ether assignment.

Supporting Information (SI) Figures and Tables

SI Figure S-1. Example structures detailing acyl, alkyl ether, and vinyl ether *sn*-1 structural configurations for lyso PE and PE. A.) *sn*-1 acyl configuration showing lyso PE(16:0/0:0), referred to as LPE(16:0) and diacyl PE(16:0/20:4); B.) *sn*-1 alkyl ether configuration showing lyso PE(O-16:0/0:0), referred to as LPE(O-16:0) and alkyl ether PE(O-16:0/20:4); C.) *sn*-1 vinyl ether configuration showing lyso PE(P-16:0/0:0), referred to as LPE(P-16:0) and vinyl ether PE(P-16:0/20:4).

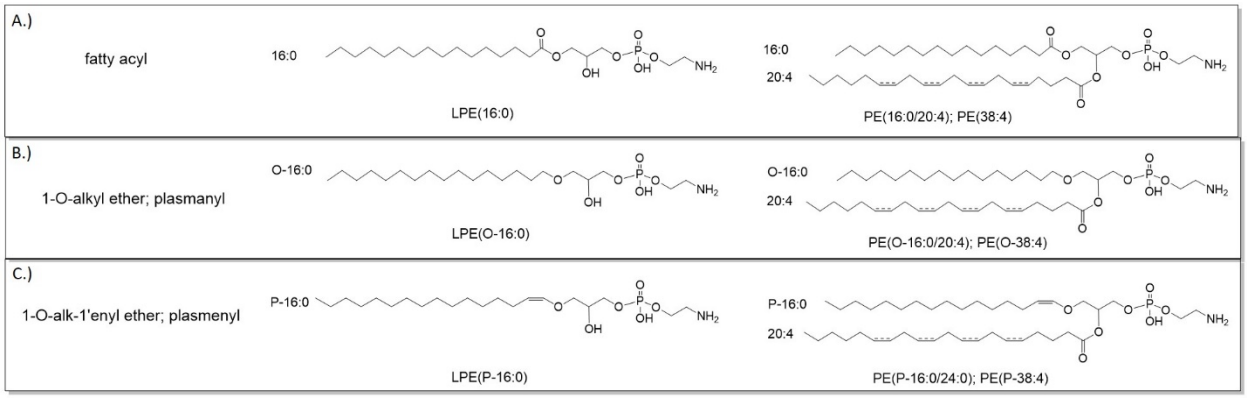

SI Figure S-2. Chromatographic separation of lysosomal lipid extracts in positive ion mode. A.) Reverse phase C18 UPLC, positive ion mode TIC of total lipid extract from mouse brain lysosomes. Several abundant peaks are labeled with putative lipid identification. B.) EIC of *m/z* values corresponding to identified PE and PE-P. Retention time and *m/z* value are listed next to the EIC peak. C.) Table with lipid ID, adduct, *m/z* value with mass error, CN, DB, ECN, and t_R for each identified PE and PE-P from the EIC.

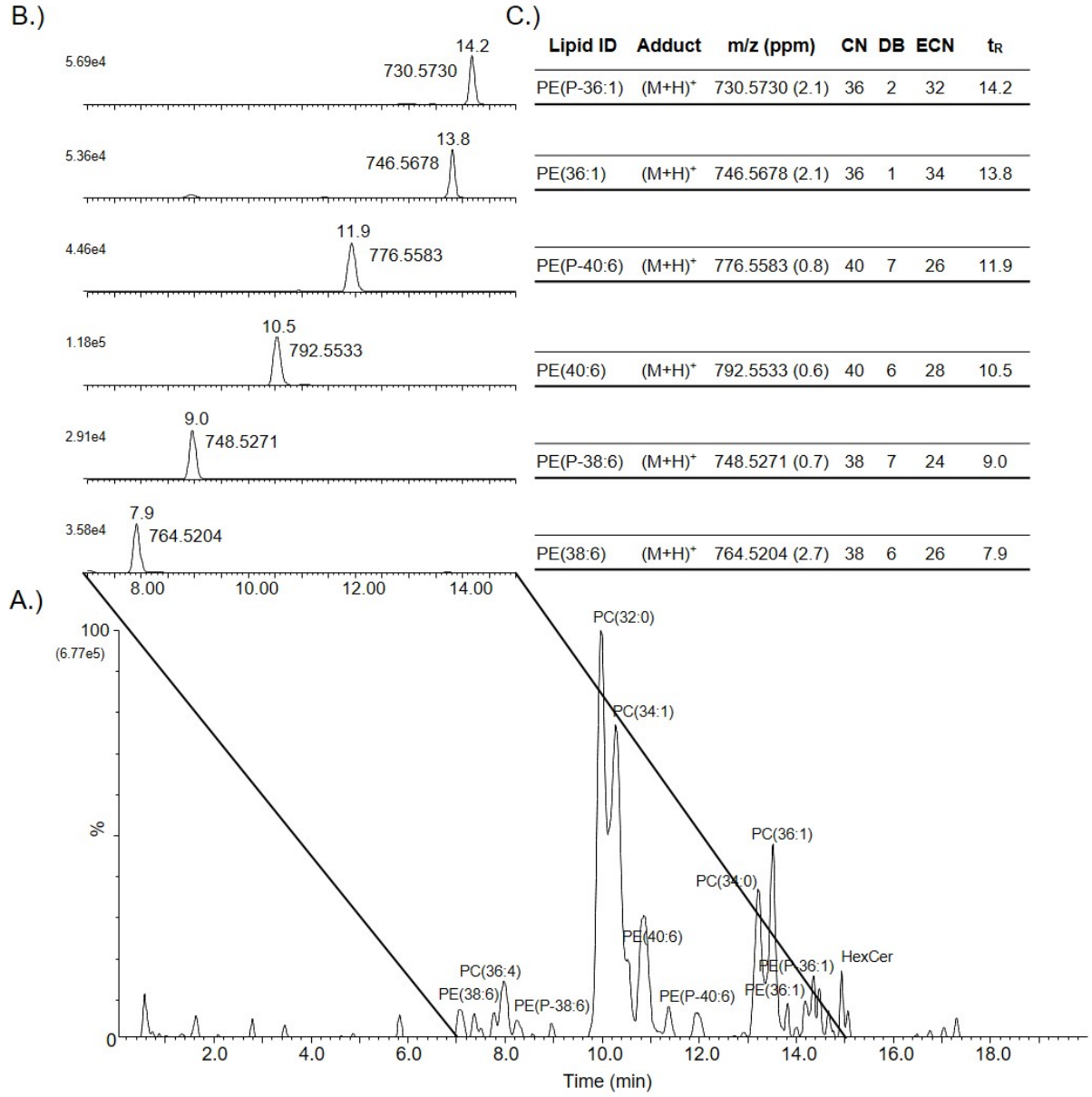

C.)

Lipid ID	Adduct	m/z (ppm)	CN	DB	ECN	t_R
PE(P-36:1)	$(M+H)^+$	730.5730 (2.1)	36	2	32	14.2
PE(36:1)	$(M+H)^+$	746.5678 (2.1)	36	1	34	13.8
PE(P-40:6)	$(M+H)^+$	776.5583 (0.8)	40	7	26	11.9
PE(40:6)	$(M+H)^+$	792.5533 (0.6)	40	6	28	10.5
PE(P-38:6)	$(M+H)^+$	748.5271 (0.7)	38	7	24	9.0
PE(38:6)	$(M+H)^+$	764.5204 (2.7)	38	6	26	7.9

SI Figure S-3. UPLC separation of authentic standards of diacyl PE and vinyl ether PE. C18 UPLC separation of diacyl and vinyl ether PE authentic standards in the positive ion mode on a Waters G2S SYNAPT. Peaks are labeled with lipid ID, t_R (min), and precursor ion *m/z* value. Inset table lists lipid ID, adduct, *m/z* value, mass accuracy (ppm), aliphatic chain number (CN), number of aliphatic double bonds (DB), equivalent carbon number (ECN), and retention time (t_R).

ID	Adduct	*m/z*	ppm	CN	DB	ECN	t_R
LPE(16:0)	$[M+H]^+$	454.291	4.6	16	0	16	1.3
LPE(18:0)	$[M+H]^+$	482.325	2.7	18	0	18	2.1
LPE(P-18:0)	$[M+H]^+$	466.331	3.2	18	1	16	2.5
PE(16:0/22:6)	$[M+H]^+$	764.524	1.7	38	6	26	9.0
PE(16:0/18:1)	$[M+H]^+$	718.541	3.6	34	1	32	12.9
PE(P-18:0/20:4)	$[M+H]^+$	752.554	6.6	38	5	28	13.6
PE(17:0/17:0)	$[M+H]^+$	720.554	0.4	34	0	34	13.8
PE(P-18:0/18:1)	$[M+H]^+$	730.579	6.7	36	2	32	14.2

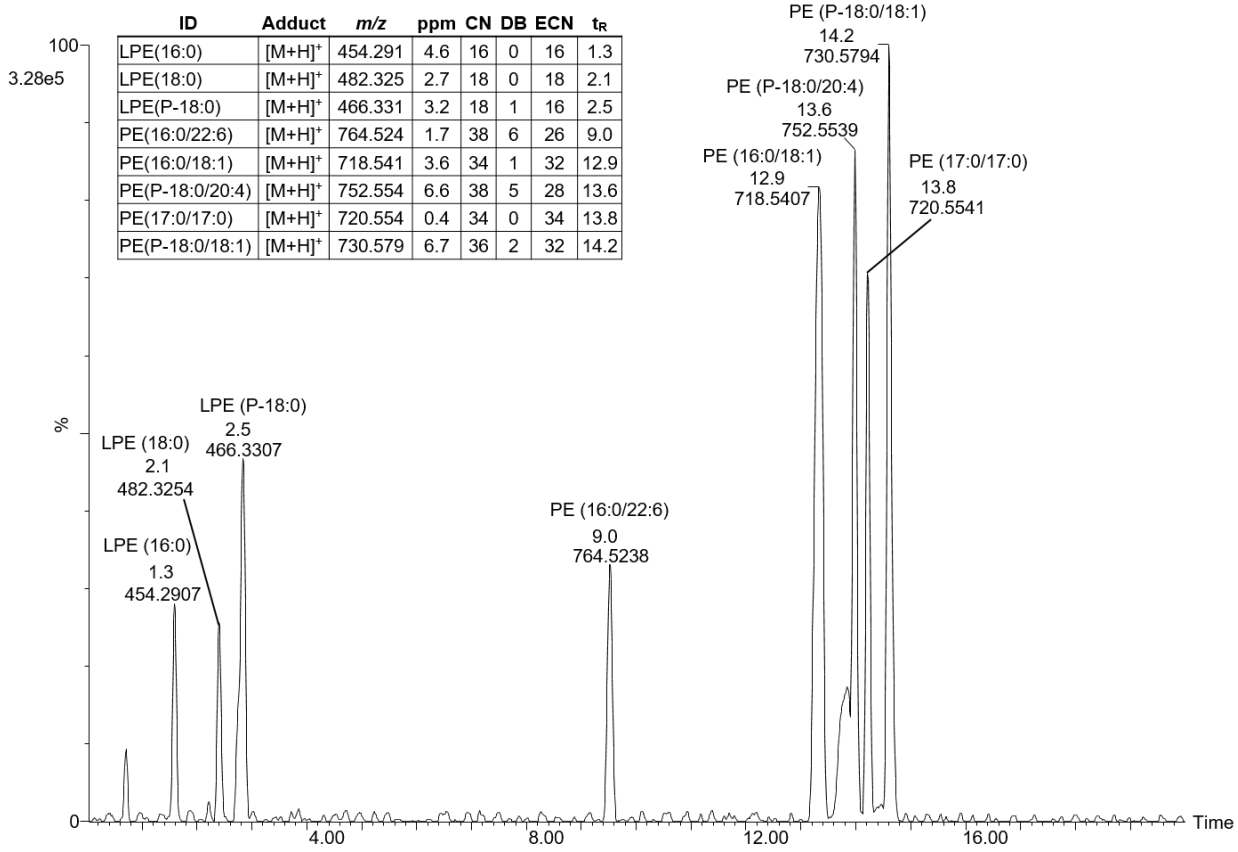

SI Figure S-4. HDMS^E-enabled structural assignment of identity for a vinyl ether PE in negative ion mode. Negative ion mode tandem mass spectrum corresponding to the elevated collision energy scan (HDMS^E) for PE(P-18:0/18:1) (*m/z* value, 728.5641; t_R, 14.2 min; drift time bin threshold <2%). Product ions observed corresponding to the neutral loss of the sn-2 acyl chain as a ketene (-18:1 (ket), *m/z* 446.3) or a free fatty acid (-18:1 (fa), *m/z* 464.3). The third product, *m/z* 281.3, corresponded to a deprotonated 18:1 acyl chain. Proposed structure is shown with likely fragmentation. Product ions were assigned based on accurate mass measurements and authentic standard verification (SI Figure 5). The double bond location on the *sn*-2 acyl chain is denoted as a dashed line indicating the double bond position was not determined.

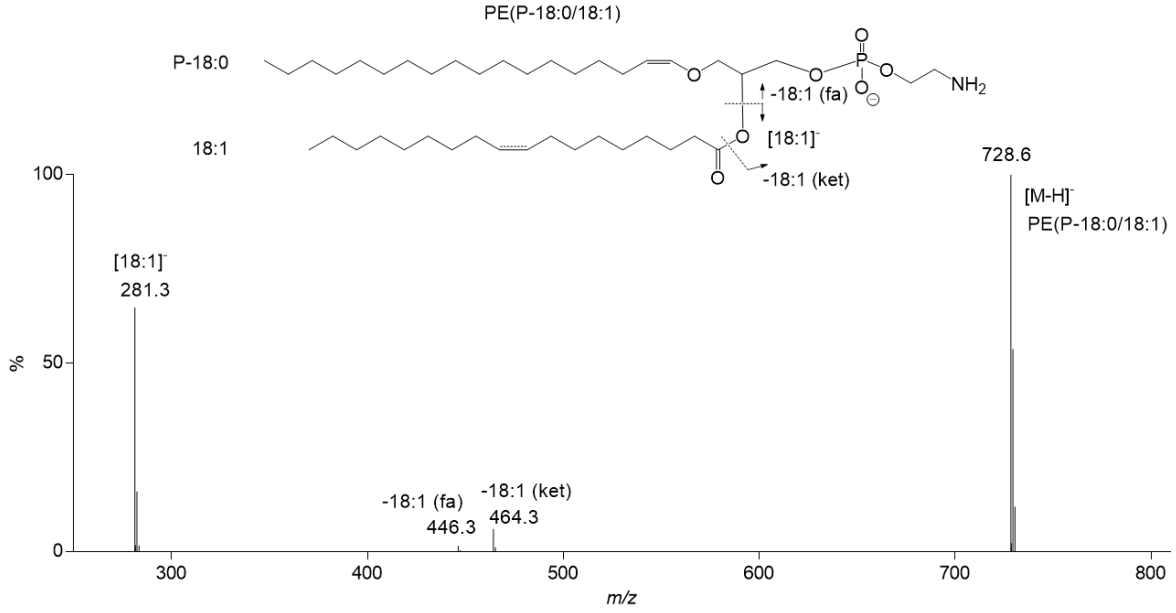

SI Figure S-5. Tandem MS spectra for an authentic diacyl PE standard (PE(18:0/18:1)). CID of a diacyl PE standard (PE(18:0/18:1)) in negative ion mode (A) and positive ion mode (B). Tandem mass spectra were recorded using UPLC-HDMS^E on a Waters G2S SYNAPT following experimental protocol outlined for data acquisition in the methods section. Inset lipid structures show likely fragmentation and correspond to product ions in spectra. Negative ion tandem mass spectrum (A) shows fragmentation at both the *sn*-1 and *sn*-2 acyl chain positions. Positive ion tandem mass spectrum (B) shows primary dissociation happens via the neutral loss of the PEtN headgroup. The double bond location on the *sn*-2 acyl chain is denoted as a dashed line indicating the double bond position was not determined.

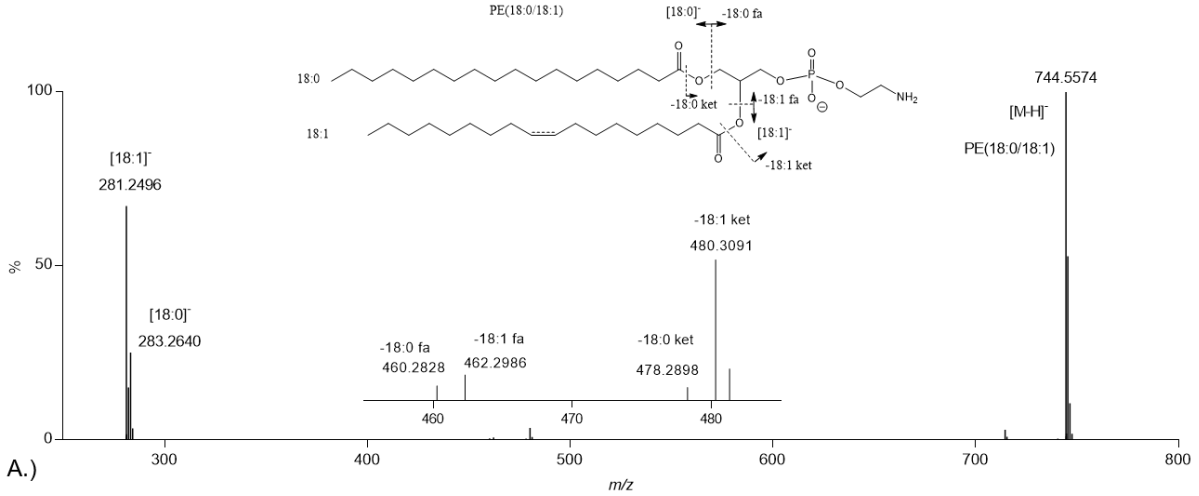

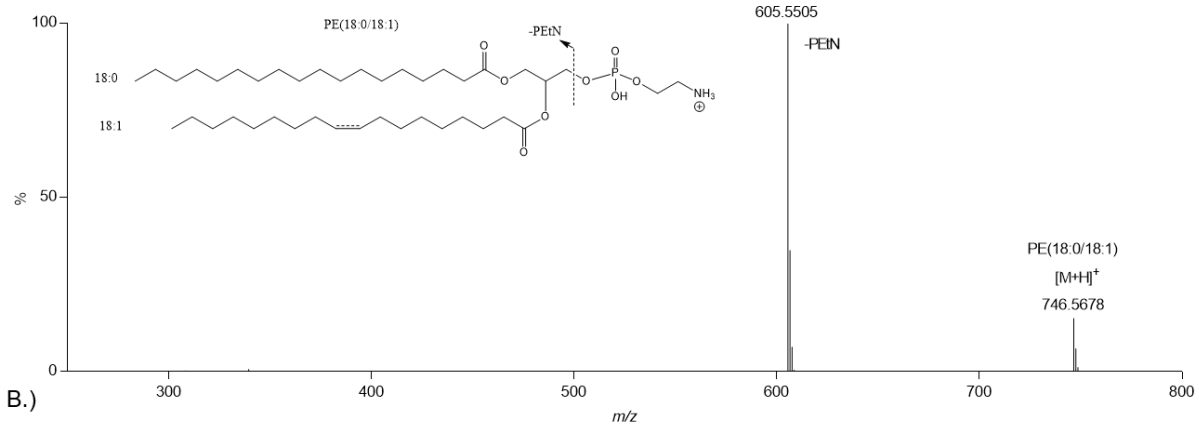

SI Figure S-6. Tandem MS spectra for an authentic vinyl ether PE standard (PE(P-18:0/18:1)). Authentic standard verification of PE(P-18:0/18:1). CID of PE(P-18:0/18:1) in negative ion mode (A) and positive ion mode (B). Tandem mass spectra were recorded using UPLC-HDMS^E on a Waters G2S SYNAPT following experimental protocol outlined for data acquisition in the methods section. Negative ion tandem mass spectrum (A) shows fragmentation at only the *sn*-2 acyl chain position. There were no observable product ions associated with fragmentation at the vinyl ether aliphatic chain on the *sn*-1 position. Refer to SI Figure S-3 for proposed structure fragmentation. Positive ion tandem mass spectrum (B) displayed low abundant product ion associated with neutral loss of PEtN (*m/z* 589.6) in contrast to diacyl and alkyl ether PE. Diagnostic product ions associated fragmentation at the *sn*-1 and *sn*-2 position are observed and are unique to vinyl ether PE. Refer to Figure 3 (main text) for proposed fragmentation.

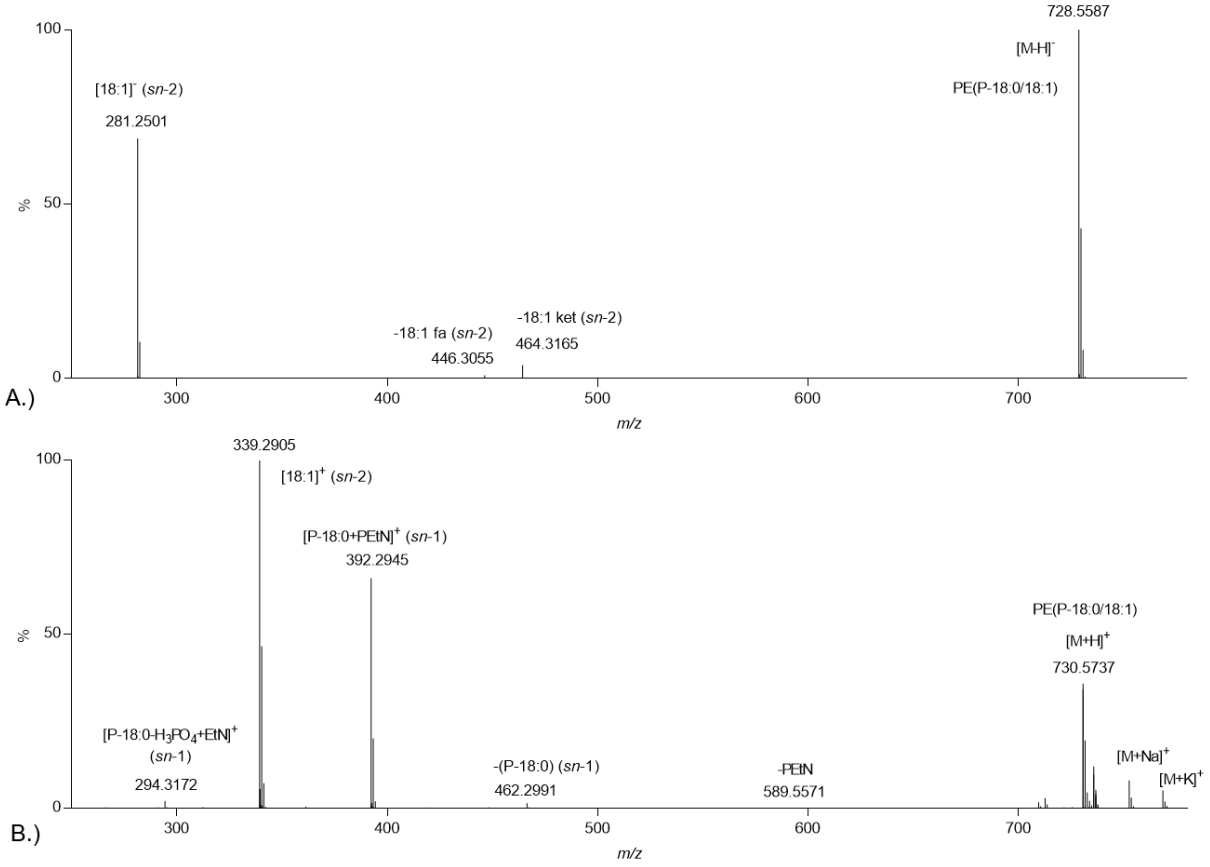

SI Figure S-7. HDMS^E tandem mass spectra of an alkyl ether PE. A.) Negative ion mode tandem mass spectrum corresponding to the elevated collision energy scan (HDMS^E) for PE(O-16:0/22:6) (*m/z* value, 748.5290; t_R, 9.4 min; drift time bin threshold <2%). B.) Positive ion mode tandem mass spectrum corresponding to the elevated collision energy scan (HDMS^E) for PE(O-16:0/22:6) (*m/z* value, 750.5432; t_R, 9.4 min; drift time bin threshold <2%). Product ions were assigned based on accurate mass measurements and literature precedent. The inset structures shows likely product ion fragmentation. The double bond locations on the *sn*-2 acyl chain are denoted as dashed lines indicating the double bond positions were not determined.

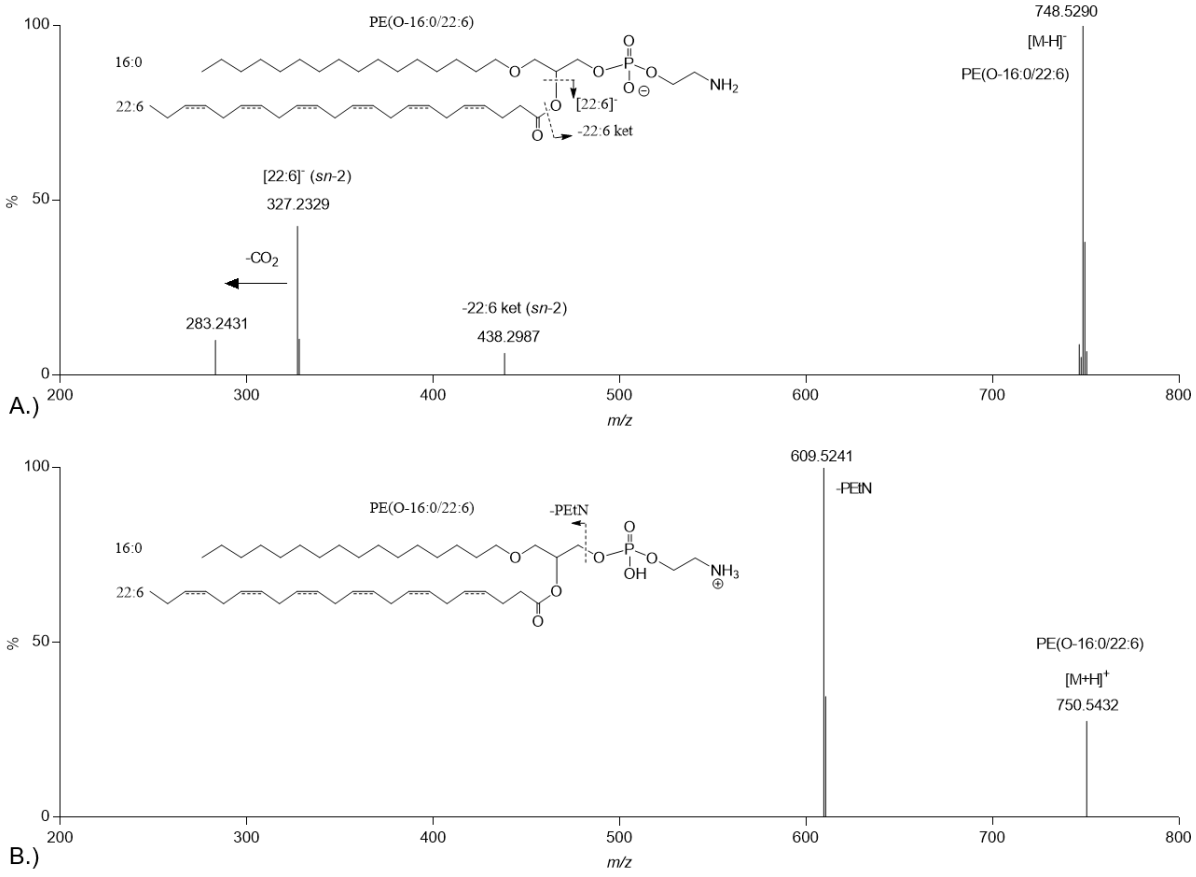

SI Table S-1. Differentially abundant brain lysosomal ether PE lipids after TBI. Analysis of ether PE lipids by UPLC-HDMS^E as described for purified cortical lysosomes from sham and TBI at 1 h after injury. SD = standard deviation, SEM = standard error of mean, CV = coefficient of variation, Significance determined using a student t-test, * p<0.05, ** p<0.01, *** p<0.005, **** p<0.0001.

					Sham (Normalized Abundance)				TBI (Normalized Abundance)					
m/z [M+H]$^+$	Lipid ID	Lipid Structure	Highest Mean	N	Mean	SD	SEM	CV	Mean	SD	SEM	CV	Significance	p value
748.5267	PE(P-38:6)	PE(P-16:0/22:6)	Sham	4	170145.4	21264.0	10632.0	12.5	115477.1	15452.9	7726.5	13.4	**	0.0059
724.5266	PE(P-36:4)	PE(P-16:0/20:4)	Sham	4	45003.3	6221.0	3110.5	13.8	28842.3	2083.3	1041.6	7.2	***	0.0026
750.5418	PE(O-38:6)	PE(O-16:0/22:6)	Sham	4	18836.5	2556.2	1278.1	13.6	11866.1	1222.9	611.4	10.3	***	0.0027
776.5583	PE(P-40:6)	PE(P-18:0/22:6)	Sham	4	246600.6	9755.7	4877.9	4.0	218844.0	11609.4	5804.7	5.3	*	0.0106
752.5574	PE(P-38:4)	PE(P-18:0/20:4)	Sham	4	67182.1	1820.9	910.4	2.7	62155.5	1444.0	722.0	2.3	***	0.0050
804.5886	PE(P-42:6)	PE(P-20:0/22:6)	Sham	4	9435.7	1397.1	698.5	14.8	6415.0	639.7	319.9	10.0	**	0.0077
702.5437	PE(P-34:1)	PE(P-16:0/18:1)/PE(P-18:1/16:0)	Sham	4	61241.1	6172.1	3086.1	10.1	52131.4	3336.0	1668.0	6.4	*	0.0408
754.5733	PE(P-38:3)	PE(P-18:0/20:3)	Sham	4	8800.2	1036.8	518.4	11.8	6755.8	1056.9	528.5	15.6	*	0.0328
780.5873	PE(P-40:4)	PE(P-18:0/22:4)	Sham	4	75026.6	8199.5	4099.7	10.9	60046.6	3303.1	1651.5	5.5	*	0.0147
756.5886	PE(P-38:2)	PE(P-18:1/20:1)	Sham	4	48667.1	6147.4	3073.7	12.6	37421.0	5432.0	2716.0	14.5	*	0.0337